

ALMA MATER STUDIORUM  
UNIVERSITÀ DI BOLOGNA

Scuola di Scienze  
Corso di Laurea in Scienze Ambientali

**VORTEX DYNAMICS IN THE  
MEDITERRANEAN SEA:  
THE IONIAN SEA CASE**

Tesi di Laurea in Oceanografia Fisica

**Relatore:**  
Prof.ssa NADIA PINARDI

**Presentata da:**  
ELISA ROMANELLI

**III sessione  
Anno Accademico 2013/2014**



*this thesis is dedicated to my parents  
for their support and encouragement*

# Acknowledgment

First and foremost, I have to thank my parents for their love and support, thank you both for giving me the possibility and the strength to reach for my goals and chase my dreams. My sister Giulia and Arturo deserve my wholehearted thanks as well.

I would like to sincerely thank my supervisor Prof.ssa Nadia Pinardi for her guidance and support throughout this study, I believe I learned from the best.

I would also like to thank Dr. Luca Giacomelli, without him this project would not have existed and the SiNCEM group, it has been a pleasure spend time with you.

To all my friends, thank you for your understanding and encouragement. Your friendship makes my life richer.

A special thanks to my professors, I have learn a lot in these three years and your infinite passion for science has fed my knowledge and my curiosity.

# Abstract

A study of the dynamics of two vortices of the Ionian Sea, the Pelops Gyre and the Western Cretan Cyclonic Gyre, is presented based upon a reanalysis dataset of the Mediterranean Sea which allows a reconstruction of the circulation structures from 1995 to 2004.

The temperature field averaged on the 10 years allowed to identify and locate the two vortices and to show that the horizontal velocity field for the cyclonic Cretan Gyre and the anticyclonic Pelops Gyre is in agreement with previous studies. In the period from 1995-2004, the two vortices are found to be recurrent: the Pelops Gyre is characterized by large interannual variability while the Cretan Gyre is more permanent but weaker. The analysis of the mean sea level variations in the area showed a large seasonal cycle attributable to the steric sea level changes in turn due to seasonal heat fluxes variability.

Finally, the satellite chlorophyll concentration has been superimposed to the circulation structure of the two gyres and, as expected, chlorophyll concentrations are higher in the Cretan cyclone and lower in the Pelops anticyclone. This is due to the dominating upwelling (downwelling) processes acting in the core of the cyclonic (anticyclonic) gyre structures.

# Contents

<b>1</b>	<b>Introduction</b>	<b>6</b>
1.1	The Mediterranean Sea circulation . . . . .	6
1.2	The Eastern Mediterranean Sea . . . . .	9
1.3	The Ionian Sea . . . . .	11
1.4	Thesis Objectives . . . . .	13
<b>2</b>	<b>Data sets and methods</b>	<b>14</b>
2.1	Description of the data set . . . . .	14
2.1.1	Reanalysis data technique . . . . .	14
2.1.2	MyOcean reanalysis . . . . .	17
2.2	Statistical analysis . . . . .	20
<b>3</b>	<b>Vortex Dynamics</b>	<b>21</b>
3.1	Introduction . . . . .	21
3.2	Temperature . . . . .	24
3.3	Velocity Structure . . . . .	28
3.4	Sea Surface Height . . . . .	33
3.5	Chlorophyll currents . . . . .	34
<b>4</b>	<b>Conclusions</b>	<b>37</b>
	<b>Bibliography</b>	<b>37</b>

# Chapter 1

## Introduction

### 1.1 The Mediterranean Sea circulation

The Mediterranean Sea is a mid-latitude, semi-enclosed sea that exchanges water, salt and heat with the North Atlantic Ocean. It is bounded by the coasts of Europe, Africa and Asia, from the Strait of Gibraltar on the west to the Dardanelles and The Suez Canal on the east (International Hydrographic Organization); its longitudinal extension is approximately 3865 *km* and its surface area is about 2 512 300sq *km*<sup>2</sup>.



Figure 1.1: Mediterranean Sea morphology and its major seas and areas

The Mediterranean Sea can be divided into two nearly equal size, anti-estuarine sub-basins known as the Western Mediterranean Basin and the Eastern Mediterranean Basin that are connected by the Strait of Sicily. Both can be also subdivided into several smaller water bodies (see Fig.1.1): the Western Mediterranean, 2500 to 3500 m in depth, contains the Alboran Sea, the Catalan Sea and the Tyrrhenian Sea while the Eastern Mediterranean, 4000 to 5000 m in depth, includes the Adriatic and the Aegean Sea, the Ionian Sea and the Levantine Basin.

Generally speaking, the Mediterranean Sea can be considered the cradle of a notable number of processes and interactions and due to its size it is found to be governed by large-scale ocean dynamics (Robinson 1992).

Its circulation, which complexity is also due to the climatic conditions, the basin geometry and bathymetry, is strongly forced by:

- Wind stress. The horizontal force of the wind on the sea surface that affects the cyclonic circulation in the northern part of the sea and the anticyclonic one in the south and therefore is responsible for the permanent gyres of the basin (Pinardi and Masetti 2000);
- Buoyancy flux. The sum of the heat and water fluxes: changes in energy stored in the upper ocean result from an imbalance between input and output of heat through the sea surface. This transfer of heat across or through a surface is called heat flux. The flux of heat and water also changes the density of surface waters, and hence their buoyancy;
- Water exchange through the various straits (Robinson 2001). The Mediterranean Sea is a concentration basin where evaporation exceed precipitation and rivers runoff (Nittis, Pinardi and Lascatatos 1993) and where the inflow-outflow system at Gibraltar controls the salt and mass budgets of the entire basin. In practice as described by Pinardi and Navarra (1993), the low-salinity Atlantic water, that enters from Gibraltar at the surface, after being transformed by intense air-sea interactions, exits deeper and saltier into the Atlantic Ocean. This process accomplished by large-scale thermal and evaporative fluxes, vertical turbulent mixing and regional deep and intermediate water masses formation processes, occurs seasonally in both the western and eastern basin and often generates coherent vortices in several parts of the basin (Isern-Fontanet 2005).

In order to describe the horizontal and vertical circulation of the Mediterranean Sea, its water masses i.e. bodies of ocean water with a distinctive

narrow range of temperature and salinity and a particular density resulting from these two parameters, must be identified and displayed.

The Mediterranean water mass formation cycle is due to the entering from the Strait of Gibraltar of the Atlantic Water (AW) which after being confined to a surface layer (50-100 m), spreads eastward from the Strait of Sicily as Modified Atlantic Water (MAW) and overlies the Levantine Intermediate Water (LIW). The MAW maximum salinity goes from 36.5 psu to 38.5 psu however during its path due to the fact that the evaporation process exceeds the precipitation one, it becomes cooler, saltier and denser therefore it tends to sink (Millot 2005). As regards the Levantine Intermediate Water (LIW), it appears regularly in the Levantine Basin especially in its north-west part (the Rhodes cyclonic gyre area) where it is formed in winter by the convective mixing caused by strong and dry continental winds. It is located at a range of depth between 150 m to 400 m where the salinity is higher than the one of the AW with a range that goes from 38.95 psu to 39.05 psu. In the southern Mediterranean, the waters produced by LIW tend to sink down to a depth of 300-400 m (Ovchinnikov and Plakhin 1984), then spread throughout the basin over the intermediate depths of both Eastern and Western Mediterranean basins and contribute to the outward flow from Gibraltar to the Atlantic ocean.

The surface circulation cell just described is part of two other internal cells of deep circulation known as the "Mediterranean Conveyor Belts" driven by the deep water masses formed in the two Mediterranean basins: the Western Mediterranean Deep Waters (WMDW) and the cooler and less saline Eastern Mediterranean Deep Waters (EMDW) (Fusco et al., 2003).

Previous studies conducted by Madec et al., (1991) and Roether and Schlitzer (1991) have shown that the former is generated in The Gulf of Lion while the latter is generated in the southern Adriatic Sea. The EMDW, which main source is the Adriatic Deep Water (ADW), occupies the abyssal layers below 1600 m depth while the one between 700 m and 1600 m is occupied by a transitional water mass which properties are intermediate between the LIW and EMDW ones.

Nevertheless, it has been observed that the movement and the transformation of the water masses are the result of three different scales. As suggested by Robinson (1992), the Mediterranean Sea general circulation can be easily described as composed of three predominant and interacting spatial scales: the basin scale, the sub-basin scale and the mesoscale. The former includes the thermohaline vertical circulation, water masses formation, mixing and dispersion. As can be seen in Fig.1.2, its superficial branch constituted by the Atlantic waters flow that enters from the Straits of Gibraltar and crosses

the Levantine Basin, forms the Algerian Current in the Western Basin and the Mid-Mediterranean Jet (MMJ) in the eastern one; its return path is fed by the westward flow of the intermediate and deep waters that are formed in the southern Adriatic and Aegean Sea. Therefore the overall cell consists of long time scale where its surface and deep branches turn out to be permanent patterns of the Mediterranean circulation. The sub-basin scale circulation is characterised by semi-permanent gyres linked by jets and coastal currents while the mesoscale activity is composed of energetic signals with scale from a few km up to 200 km, instabilities of coastal currents and off-shore eddies characterised by both inter-annual variability and infra-seasonal variations (Ayoub 1997 and Pinardi 2013).

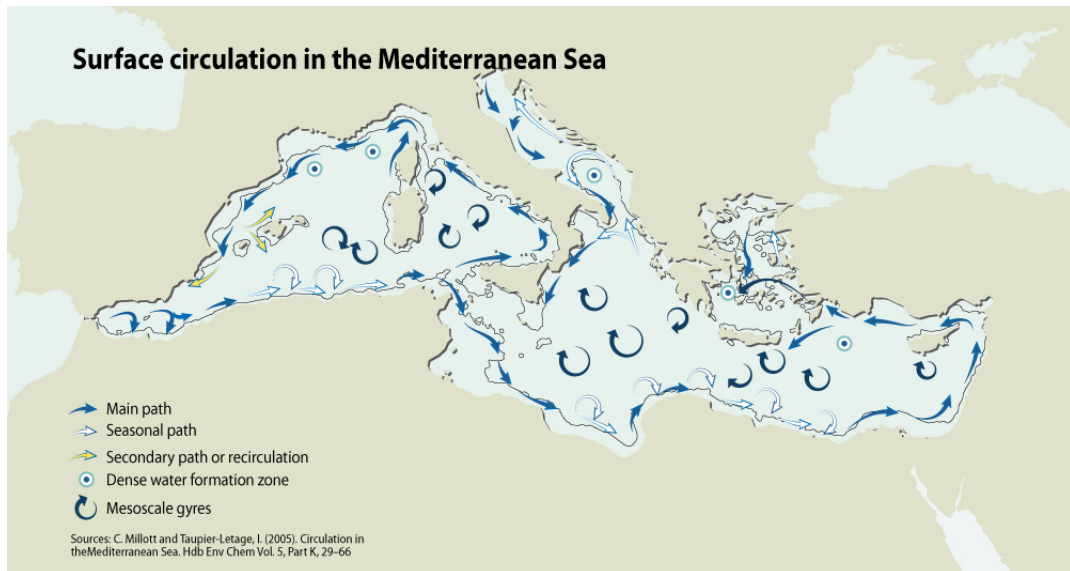


Figure 1.2: Surface circulation in the Mediterranean Sea

## 1.2 The Eastern Mediterranean Sea

The Eastern Mediterranean Sea is an isolated sub-basin bounded by the Western Basin on the west, by the Dardanelles on the north, by the Suez Canal on the south and by Syria and Palestine on the east. Its circulation is complex due to multiple forcings and water mass formations but, as already seen previously, it can be more simply described as composed of three spatial scales (see Fig.1.3).

A study conducted by Robinson et al., (1992) shows that the thermohaline

circulation of the Eastern Basin consists of two cells: a single vertical cell that flows throughout the Ionian Sea and the Levantine Basin with a turn over time for deep water of about 126 years and the external cell that involves the exchange of water between the Mediterranean Basins and the AW. As regards the sub-basin scale, it is composed by gyre and permanent or semi-permanent cyclonic and anticyclonic structures which patterns are linked by jets and meandering currents; specifically, the Mid-Mediterranean Jet result to be fed by the jet of Atlantic Water that enters from the Sicily Strait, continues its path in the central Levantine Basin and separates itself into two main branches: one flows to Cyprus and the other turns southward. In addition both permanent and recurrent structures have been found and seem to be the consequence of factors as topography and seasonal wind-stress that create large-scale forcing structures. The sub-basin scale circulation interacts with the mesoscale eddies, meanders and oscillations that occur stronger in the Levantine Basin.

Furthermore, several mechanisms that influence the Eastern Mediterranean circulation have been identified: climate processes that regard both intermediate and deep water masses, salt concentration that is involved in the formation of the internal deep water, thermal and evaporation fluxes that drive the circulation of the Eastern Levantine Basin and the wind-stress curl that impose the seasonality of the Ionian Sea structures.

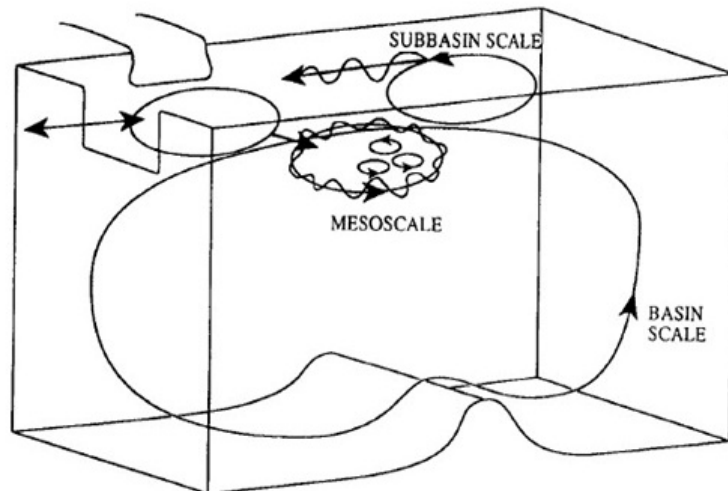


Figure 1.3: Scales of circulation variabilities and interactions in the Eastern Mediterranean Sea (Robinson et al., 1992)

### 1.3 The Ionian Sea

The Ionian Sea is a sub basin of the Mediterranean Sea located in the Eastern Mediterranean Basin; it is bounded by southern Italy and Albania on the north, by western Greece on the east and by northern Africa on the south. To the west it communicates with the Western Mediterranean through the Strait of Sicily, to the east with the Levantine Basin through the Cretan Passage and with the Aegean Sea through the Kithira Strait and finally to the north with the Adriatic Sea with the Strait of Otranto.

The Ionian Sea has been described by Malanotte-Rizzoli (1997) as the transition basin for the spreading of the deep thermohaline cell from its source in the southern Adriatic, to the Levantine Basin. Specifically the ADW exits from the Otranto Strait and due to the constrain imposed by the conservation of potential vorticity, spreads into the Ionian abyssal layers and then became transform into EMDW. In addition, the Ionian Sea exchanges water properties in the east with the Levantine Basin through the Cretan Passage and in the northeast with the Aegean Sea through the Western Cretan Arc Strait. Thus it can be considered a transitional basin for all the water masses of the Eastern Mediterranean.

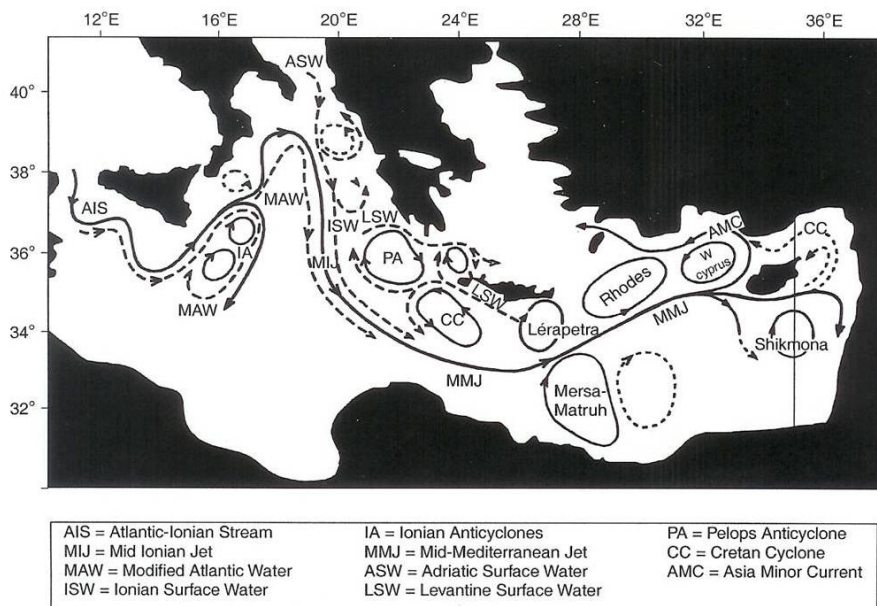


Figure 1.4: Surface circulation in the Eastern Basin and the Ionian Sea (Robinson and Golnaraghi 1994)

The Ionian Sea circulation is characterised by three main water masses:

1. The MAW. It enters the Ionian Sea from the Strait of Sicily where it can be identified as a subsurface minimum of salinity between 20 and 100 m depth (Nittis et al., 1993), then it is carried into the basin interior in the surface layer by the Atlantic-Ionian Stream (AIS) that reaches the Cretan Passage to become the MMJ. The MAW signal is expected to be stronger during summer because of the greater intensity of evaporation and the lower mixing;
2. the LIW. It is formed by the intense evaporation and mixing processes of the MAW that occurs in the Levantine basin. The LIW enters the Ionian Sea through the Cretan Passage and, as previously mentioned, has a maximum salinity at intermediate depth. In the Ionian Sea it is denser due to the decrease of temperature and the increase of salinity;
3. and, the EMDW. It lies at a depth of 1200 m and shows less saline and cooler waters than the LIW; it characterises the intermediate and deep circulations.

As shown by Malanotte-Rizzoli (1997), the paths of these water masses are determined by the advection, the strong jet-like currents in the surface layers, and the veering induced by cyclonic and anticyclonic structures around their areas.

Furthermore other two features are considered important in order to display the Ionian Sea general circulation:

- The Ionian Surface Water (ISW): which can be differentiated by the MAW because in the surface layer during summer it is saltier and warmer. In fact as noticed by Nittis et al., (1993) its salinity profile shows a well developed mixed layer; the ISW masses are formed by intense air-sea interaction processes occurred in the summer months.
- The AIS: an intense surface circulation that characterises the central-western Ionian Sea. As previously described, it determines by advection the spreading of the MAW from the Strait of Sicily in the near-surface layer. The AIS-MAW jet so formed bifurcates into two main branches: one branch turns southward and forms overall an anticyclonic area while the second branch is more evident in the northeastern part advecting the MAW, after that it turns southward and crosses the Ionian Basin advecting the MAW on its right side and the ISW on its left. Finally it veers to the east and enters the Cretan passage where it became the MMJ that remains confined in the central region of the Ionian

Sea. Pinardi et al., (2013) have found that before 1997 the AIS was occupying the northern Ionian Sea, producing an overall anticyclonic circulation structure, while after 1997 it remains in the middle of the Ionian Basin and a cyclonic gyre develops at its northern limits. This is a current reversal phenomenon known as the "Northern Ionian Reversal phenomenon" that has emerged to be driven by wind and provoked by the excursion of the AIS from the middle to the northern parts of the basin.

The main tendency of the Ionian Basin is an overall cyclonic circulation in winter and a more complicated circulation pattern with the occurrence of several transient gyres in the other seasons (Larnicol et al.,1995). According to Pinardi and Navarra (1993), the main source of the Ionian Sea circulation variability is the local wind changes; they also conclude that the southern Ionian basin is more sensitive to the remote forcing from the Levantine Basin than the northern one.

Therefore, the mean flow is not very well defined, except for a few sub-basin scale structure such as the permanent Pelops Gyre that is located on the north-eastern side of the AIS (Robinson et al., 1992).

Many aspects of the Ionian Sea circulation remain unknown and several investigations still have to be carried out.

## 1.4 Thesis Objectives

The general objective of the present study is the analysis of the dynamics of two vortices of the Ionian Sea: the Pelops Gyre and the Western Cretan Cyclonic Gyre.

This thesis is organized as follow: in Chapter 2 data processing and datasets are presented, in addition the statistics have been detailed. Chapter 3 is mainly devoted to presenting the results: in the first section, a brief introduction about the geostrophic currents and their cyclonic and anticyclonic movements are given; in the second section, the Pelops Gyre and the Cretan Gyre are identified and located, then the fields of temperature are analyzed. In the third section, the maps of the horizontal velocity field show the time permanence and the variability of the vortices. In the fourth section, the seasonal cycle has been shown from the analysis of the variability of the sea level height; in the last section, the chlorophyll concentration levels in the area have been analysed. Finally, in Chapter 4 the conclusions are outlined.

# Chapter 2

## Data sets and methods

### 2.1 Description of the data set

The present study has been carried out using MyOcean's MEDSEA\_REANALYSIS\_PHYS\_006\_004 that is the physical reanalysis component of the Mediterranean Sea Forecasting system model (Pinardi et al., 2003).

#### 2.1.1 Reanalysis data technique

In order to study the physical and biochemical state of the ocean, understand its past and obtain the best possible description of its circulation, scientists are using a new data assimilation process known as re-analysis where an ocean dynamic model and the historical observations are fused in order to produce the best statistical estimate of the state of the system. A reanalysis is an analysis done with a consistent model and data assimilation scheme for the period of interest yielding complete, global gridded data that are as temporally homogeneous as possible. Therefore this approach allows to obtain consistent datasets made continuous in space and time with an interpolation scheme that fills the observational gaps. Furthermore, depicting the full three dimensional state of the planet as a function of time, its products display a time series in the past which are part of the Multi Year Products category.

The data assimilation process combines two different type of data:

1. The real-time data. These are quality controlled in situ and satellite-base observations that may come from in-situ platforms as surface and sub-surface buoys and floats but are mainly collected by the Voluntary Observing Ship (VOS) system that takes and transmits the data from the ship, throughout the satellite telecommunication system (ARGO),

to the collecting centre. However due to the fact that the transmission process is in real time, the data are decimated and so they lose in accuracy and resolution. These measurements are also used to complement the satellite-based observations: after being assimilated in a numerical model they serve as a reference point for its calibration. On the other hand the satellite-base data are taken from satellite altimetry and corrected with algorithms. The reanalysis observational in situ and satellite datasets include: satellite SLA data and in situ and satellite profiles of temperature and salinity.

2. The ocean general circulation model (OGCM) outputs. In oceanography a model is a mathematical computer-generated description of physical phenomena that simulates the movement of the Earth's fluids and the consequent transport of heat and matter. An ocean model is ruled by established hydrodynamic laws along with observations, indeed as previously mentioned, an ocean model is based on in situ measurements and satellite observations; the results are equations which express ocean parameters as current, temperature and salinity as a function of time.

Lorenz in 2002 defines data assimilation as "the process of finding the model representation which is most consistent with observations".

This concept can be traced back to the least-squares method of Gauss that allows to calculate the best statistical fit between two approximations of the reality (truth): an observed value and a value provided by a model. This is accomplished by minimizing their differences in order to approximate as nearly as possible the reality and therefore the current state of the system.

Mathematically speaking, considering two independent approximations of the real state of the ocean ( $X$ ) that occur in the same location, where the former is a numerical model solution ( $X^b$ ) and the latter is an observation ( $Y^o$ ) with their respective errors ( $E^b$ ) =  $(X^b) - X$  and ( $E^o$ ) =  $Y^o - X$ , it can be assumed that the error probability distribution is Gaussian:

$$p(E) = \frac{1}{\sqrt{2\pi}\sigma} e^{-\left(\frac{E^2}{2\sigma^2}\right)} \quad (2.1)$$

where  $\sigma^2 = \langle E^2 \rangle$ . The distribution closer to reality is considered to be:

$$p(E^b)p(E^o) = \frac{1}{\sqrt{2\pi}\sigma_b\sigma_o} e^{-I} \quad (2.2)$$

with

$$I = \frac{1}{2} \left[ \frac{(X^b - X)^2}{\sigma_b^2} + \frac{(Y^o - X)^2}{\sigma_o^2} \right] \quad (2.3)$$

In order to get the maximum probability, the exponent ( $I$ ) must have a minimum value that is achieved at the best estimated value ( $X^a$ ) also called analysis:

$$X^a = X^b + \left(\frac{\sigma_b^2}{\sigma_b^2 + \sigma_o^2}\right)(Y^o - X^b) \quad (2.4)$$

where  $Y^o - X^b$  is the misfit i.e. the difference between the model solution and the observations before data insertion. Therefore  $X^a$  is the weighted average of  $X^b$  and the misfit. Actually the observations will be taken at different locations so in general the misfit can be write as:

$$d = Y^o - H(X^b) \quad (2.5)$$

where  $H$  is the observational operator and  $d, Y^o, X^b$  are vectors in the four-dimensional space.

As described by Pinardi et al. 2008, in the oceanic data assimilation systems, the best estimate is generally the state of the ocean that has the fast motion filtered out, in addition ocean is considered to be close to horizontal non-divergence and the flow is assumed to be smooth, therefore observations can provide information about the reality and the model needs to be parameterised in the sub-grid scale phenomena that will not drive the solution too far from the geostrophic balance.

In order to assess the quality and accuracy of the assimilation system, three basic indicators are used:

- Consistency indicator. It is derived from phenomenological studies or observations and indicates the qualitative correspondence of circulation structures in the analysis fields;
- Quality indicator. It shows the comparison between observations and model before data insertion. It can be expressed in terms of the root-mean-square of the misfit;
- Accuracy indicator. This indicator compares the forecast system analysis and the objective analysis which can be done with the satellite data.

## 2.1.2 MyOcean reanalysis

The reanalysis datasets of this thesis have been downloaded from the service tool MyOcean and are the products of the MED REA hydrodynamic model that is constituted by 3D, daily and monthly mean fields of Temperature, Salinity, Zonal and Meridional Velocity, and by 2D, daily and monthly mean fields of Sea Surface Height. These data are supplied by the Nucleous for European Modeling of the Ocean (NEMO), with a three-dimensional variational data assimilation scheme (OceanVar developed by Dobricic and Pinardi (2008)) for temperature and salinity vertical profiles and satellite Sea Level Anomaly along track data.

The model has an horizontal grid resolution of  $1/16^\circ$  (ca. 6-7 km) and an unevenly spaced vertical levels of 72. It is located in the Mediterranean Basin and also extends into the Atlantic in order to better resolve the exchanges with the Atlantic Ocean at the Strait of Gibraltar.

It is forced by momentum, water and heat fluxes interactively computed by bulk formulas and it predicted surface temperatures. Water balance is computed as Evaporation minus Precipitation and Runoff; the evaporation is derived from the latent heat flux while runoff is provided by monthly mean datasets. The background error correlation matrix which represents the error variance for all the model state variables and their correlation, is estimated from the temporal variability of parameters in a historical model simulation and vary seasonally in 13 regions of the Mediterranean Sea that has different physical characteristics.

The assimilated data include:

1. Sea Level Anomaly. This data set is composed of mono altimeter satellite along-track sea surface heights computed with respect to a seven-year mean.
2. In situ Temperature and Salinity profiles. These datasets have been collected from European Marine databases and have been archived in a specific format in order to be assimilated. The profiles considered for the MED REA production belong from several instrumental data type: CTDs, XBTs, MBTs, bottles, ARGO floats.

MED REA statistics computed for temperature, salinity and SLA use the misfits:

$$m = y^o - H(x) \quad (2.6)$$

where, as previously seen,  $y^o$  is the observation,  $H$  is the linearised observational operator, and  $x$  is the model solution (Adani et al., 2011). Misfits

have been computed using the background model fields before the data are assimilated. Since data are mostly sparse in space and time, the background might be considered unaffected by observations assimilated previously. The monthly mean BIAS and root mean square error (RMSE) from temperature and salinity misfits have been computed over 5 layers: L1) 0-30m; L2) 30-150m; L3) 150-300m; L4) 300-600m; L5) 600-1000. A deeper layer has not been considered because the scarce data availability does not provide enough statistical significance. The quality of MED REA system has been assessed using 26 years from 1987 to 2012.

Furthermore other two datasets have been used:

- The OCEANCOLOUR\_MED\_CHL\_L3\_REP\_OBSERVATIONS\_009\_073 which is the Mediterranean Sea surface chlorophyll concentration from multisatellite observations reprocessed. This data product files come from the MyOcean Ocean Colour Thematic Assembly Centre (OCTAC) that is a distributed subsystem which acts as a Production Centre. Its mission is to operate the European Ocean Colour operational service for GMES marine applications, providing high quality ocean colour products, accompanied by a suite of quality assurance items including accuracy. CHL is the phytoplankton chlorophyll concentration evaluated either via standard processing (the one provided by space agencies) or via region-specific algorithms. The chlorophyll product is obtained by means of the MedOC4 algorithm (Mediterranean Ocean Color 4 bands, Volpe et al., 2007) which is an empirical ocean color algorithm for chlorophyll retrieval. Ocean color technique exploits the emerging electromagnetic radiation from the sea surface in different wavelengths. The spectral variability of this signal defines the so called ocean color which is affected by the presence of phytoplankton. The data are daily composite products obtained by merging all the ocean satellite passages and they have a spatial resolution of 4 km. In addition they are reprocessed products i.e. consistent multi-year time series produced by using a consolidated and consistent input dataset, with a unique processing software configuration. Therefore they represent a much more solid data set for long-term analyses.
- The SEALEVEL\_MED\_MDT\_L4\_REF\_OBSERVATIONS\_008\_014 which is the Mediterranean Mean Dynamic Topography computed on a 7 years period (1993-1999) i.e. the mean sea surface with respect to geoid, a reference surface that reflects the major currents of the oceans. The computation is based on: - GRACE data, - altimetry data, - in-situ data (hydrologic and drifters data). The altimeter provides the

sea surface height relative to the reference ellipsoid. It is the sum of the geoid plus the dynamic topography, once removed other oceanic and atmospheric effects. By averaging altimetric heights over a given period, a Mean Sea Surface (MSS) can be estimated. The MSS is referenced to the Earth ellipsoid; MSS is the sum of the geoid  $G$  plus the mean dynamic topography MDT. Thus, by subtracting the geoid  $G$ , we can obtain the Mean Dynamic topography MDT; this is the so called "direct method". Unfortunately, geoid accuracy is poor, but can be used at large scale. The EIGEN-GRACE03S geoid is used here, where two surfaces are subtracted, to provide a large scale mean dynamic topography.

MyOcean downloaded files are NetCDF (The Network Common Data Form) files of a geographical box selected using values of longitude and latitude and time range. In this project, data are composed of daily mean values from 1995 to 2004 that provide information about five different ocean parameters: temperature, salinity, currents, sea level and chlorophyll concentration and cover a selected geographical box which longitude goes from  $18^{\circ}\text{E}$  to  $28^{\circ}\text{E}$  and latitude from  $30^{\circ}\text{N}$  to  $40^{\circ}\text{N}$  (see Fig.2.1.).

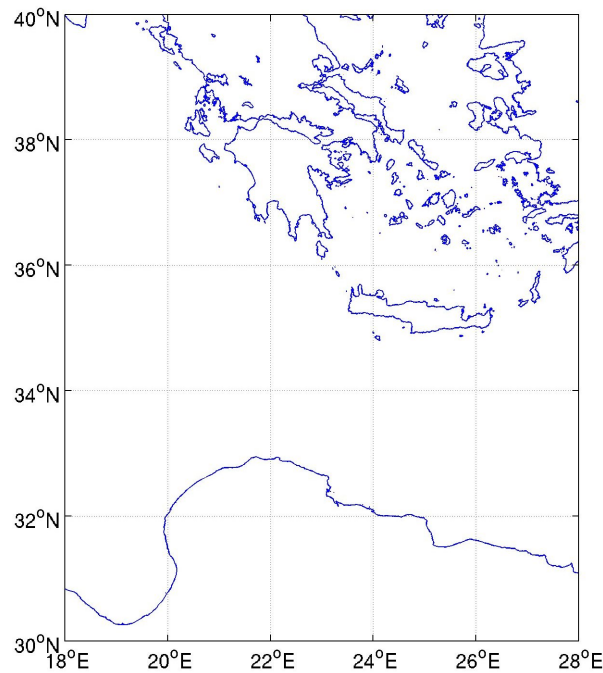


Figure 2.1: Ionian Sea area where the Pelops Gyre and the Cretan Gyre are located

## 2.2 Statistical analysis

The first step of this thesis has been to calculate a climatology for the period between 1995 and 2004 through which create maps of temperature, salinity and velocity averaged on the 10 years. These visual representations give the mean field on the 10 years and therefore allow to localize the two structures: the Pelops Gyre and the Western Cretan Cyclonic Gyre:

$$\langle X \rangle = \frac{1}{T} \int_0^T X dt \quad (2.7)$$

where  $X$  is an ocean parameter between temperature, salinity and horizontal velocity and  $T$  is the time range. Furthermore, it has been chosen to analyze different depths of the water column in order to see the variation of the consistency of the vortices in respect to the depth.

The second step was to calculate the monthly anomalies with respect to the climatology previously created. The resulting maps of anomaly are a representation of the difference between the data of February, May, August and November of each year and the climatology, indeed an anomaly describes the deviation from a properly defined mean. The anomalies have been calculated as follow:

$$X' = X - \langle X \rangle \quad (2.8)$$

where  $X$  is the monthly values averaged on the 10 years and  $\langle X \rangle$  is equation 2.7..

The third step has been to calculate the anomaly of the sea level height (SSH) to show the seasonal cycle in the area. In order to do that, the mean dynamic topography (MDT) has been subtracted to the monthly values of SSH averaged over the 10 years.

To be noticed that if the oceans were at rest covering the entire earth, then the sea surface would be a geopotential surface and so would do no work against gravity. It is therefore referred to as the geoid of the earth. Any deviations from the geoid would introduce slopes in the sea surface, which can be measured if the geoid is known. The changes in the sea surface height (or steric height) are caused by currents and therefore, it is also referred to as the dynamic topography of the ocean. The mean sea surface topography includes the geoid height.

Finally, a map of the satellite chlorophyll concentration averaged on the 10 years showed the downwelling and upwelling processes that act in the gyres core.

# Chapter 3

## Vortex Dynamics

### 3.1 Introduction

On the rotating Earth, the Coriolis force deflects the motion of the ocean currents and the acceleration ceases only when the speed,  $U$ , of the current is just fast enough to produce a Coriolis force that can exactly balance the horizontal pressure-gradient force. This balance called geostrophic balance is given as:

$$-fv_g = -\frac{1}{\rho}\left(\frac{\delta p}{\delta x}\right) \quad (3.1)$$

$$fu_g = -\frac{1}{\rho}\left(\frac{\delta p}{\delta y}\right) \quad (3.2)$$

where  $\frac{\delta p}{\delta x}$  and  $\frac{\delta p}{\delta y}$  are the horizontal pressure gradient along the x-axis and y-axis, respectively,  $u$  and  $v$  are the horizontal components of the velocity  $U$  along the x-axis and y-axis, respectively and  $f = 2\Omega \sin \varphi$  is the Coriolis parameter with  $\Omega$  as the rotation frequency of earth and  $\varphi$  the latitude. From this balance it follows that the current direction must be perpendicular to the pressure gradient because the Coriolis force always acts perpendicular to the motion.

The geostrophic balance allows to calculate the velocity field from the pressure field:

$$fv_g = \frac{1}{\rho}\left(\frac{\Delta p}{\Delta x}\right) \quad (3.3)$$

$$fu_g = -\frac{1}{\rho}\left(\frac{\Delta p}{\Delta y}\right) \quad (3.4)$$

Consequently, in the Northern Hemisphere the cyclonic motion has a counterclockwise rotation with lower pressure in its centre while the anticyclonic

motion has a clockwise rotation with higher pressure in the centre of rotation. These type of currents are called a geostrophic currents.

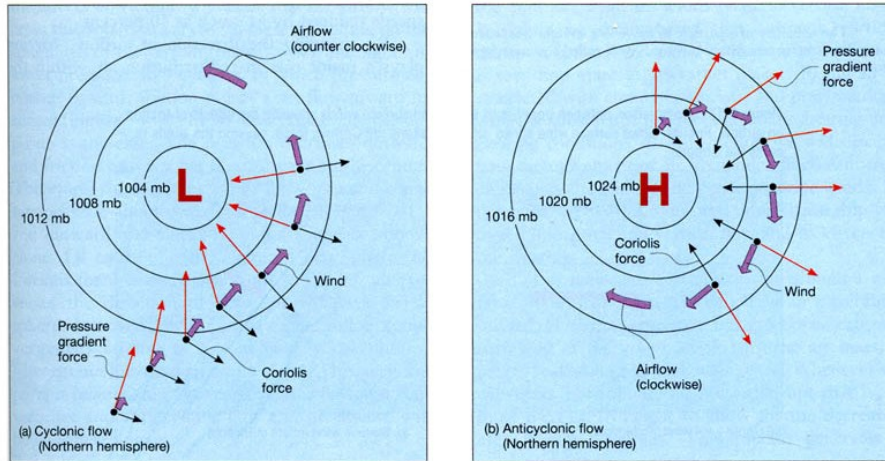


Figure 3.1: Field with isolines of equal pressure and isobars. The vectors indicate the directions of the geostrophic field in the Northern Hemisphere while in the Southern Hemisphere, the directions are reversed

At the surface, ocean circulation derives its energy from two sources: the wind stress that, inducing a momentum exchange, defines wind-driven circulation and the variations in water density imposed by exchange of ocean heat, and water with the atmosphere that induces a buoyancy exchange and drives the thermohaline circulation. Since both the sea-air buoyancy and momentum exchange are dependent on wind speed, these two circulation types are not fully independent, however the wind-driven circulation is the strongest in the surface layer and it is configured as eddies and gyres while the thermohaline circulation extends to the seafloor and forms circulation patterns that envelop the global ocean.

By definition, eddies are the result of the turbulence of the oceanic circulation. Cyclonic eddies have a shallow thermocline at the center and are therefore also known as cold-core eddies while anticyclonic eddies are associated with a depressed thermocline in the center and are also known as warm-core eddies. Generally the mesoscale eddies give an important contribute to the horizontal heat and salt transport which is mainly due to individual eddy movements. In fact temperature and salinity anomalies inside individual eddies tend to move with eddies because of advective trapping of interior water parcels. (Dong et al 2014).

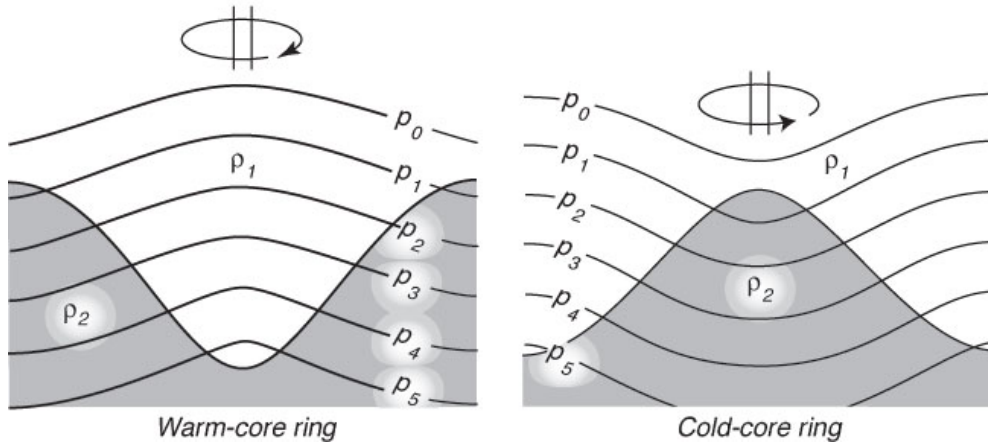


Figure 3.2: Sloping isobars in oceanic eddy circulation forced by atmospheric circulations. (a) warm core eddy: clockwise circulation with isobars sloping downwards and isopycnals upwards from the centre; (b) cold core eddy: anti-clockwise circulation; isobars slope upward but isopycnals slope downwards from the centre

Therefore, mesoscale eddies are temporary spinning flows on scales of a few hundred that can travel long distances before dissipating; on the other hand gyres are bigger wind-driven cyclonic or anticyclonic currents with a specific persistency in time.

## 3.2 Temperature

The visual representation of the temperature field averaged on the 10 years analysis (Fig. 3.3) has allowed to identify and locate the two circulation structures of the Ionia Sea known as Pelops Gyre and Western Cretan Cyclonic Gyre. The former is an anticyclone and therefore shows a warm core marked by a temperature of about  $15.2^{\circ}\text{C}$  while the latter is characterized by a cyclonic motion and thus appears colder with a temperature of about  $14.2^{\circ}\text{C}$ .

As can be seen in Fig.3.4, the Pelops gyre is located at  $36^{\circ}\text{N}$  and  $22^{\circ}\text{E}$  while the Cretan Gyre at  $35^{\circ}\text{N}$  and  $23^{\circ}\text{E}$ , in addition they both seem to have a diameter of about 120 km.

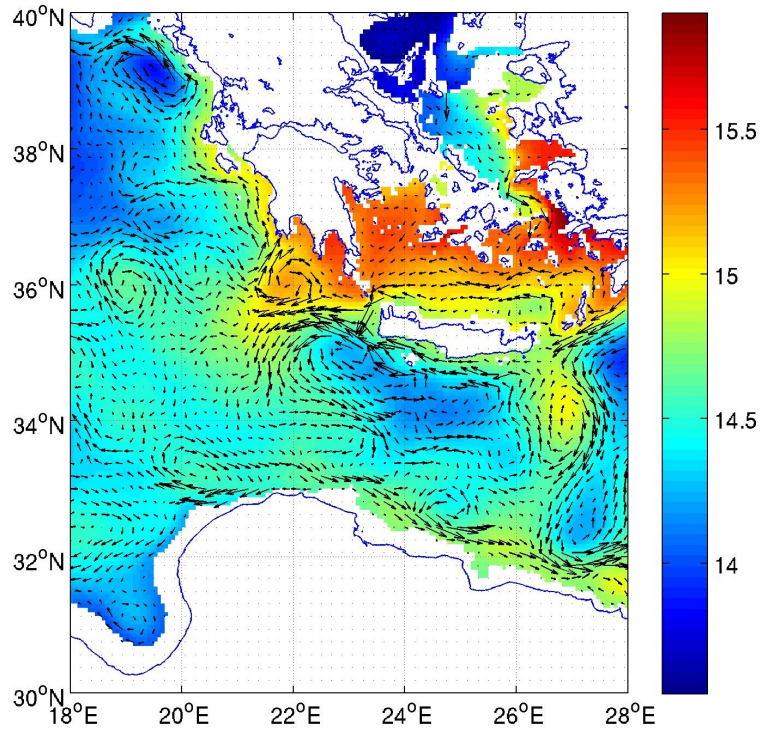


Figure 3.3: The temperature field on the 10 years at a depth of 250 m

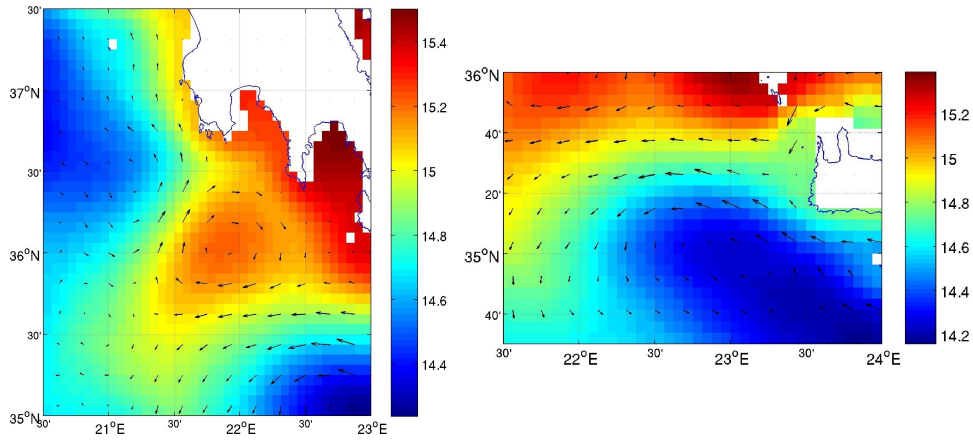


Figure 3.4: From left to right: Pelops Gyre and Western Cretan Cyclonic Gyre

Furthermore, the anomaly maps illustrate the difference between the temperature values of each year during the months of February, May, August and November and the mean temperature value on the 10 years. The attention has been focused on these four months because they are considered valid detectors of the main characteristics of the sea during the seasonal cycle. By observing the maps, it can be noticed that the absolute value of anomaly is almost always of 2 degree which means that, in general, the mean temperature of each months has undergone changes that can be compared. Specifically, the Pelops Gyre shows positive anomalies compared to the Cretan gyre that is characterized by negative ones (see Fig.3.5). This is consistent with the fact that cyclonic gyres have a shallow thermocline at the center while anti-cyclonic gyres are associated with a depressed one.

By plotting the temperature anomaly, it appears evident the seasonal cycle at small depths (15 m) where the consistency of the gyres is influenced by disturbing factors that occur at the surface (see Fig.3.6). On the other hand, the interannual cycle is more clear at bigger depths (250 m) where the seasonal one is weaker (see Fig.3.7 and 3.8). It has been chosen to consider these two different depths of the top layer of the water column in order to demonstrate that the 15 m depth layer is the most strongly influenced by the atmospheric forcing and therefore the more capable of amplifying the seasonal variability.

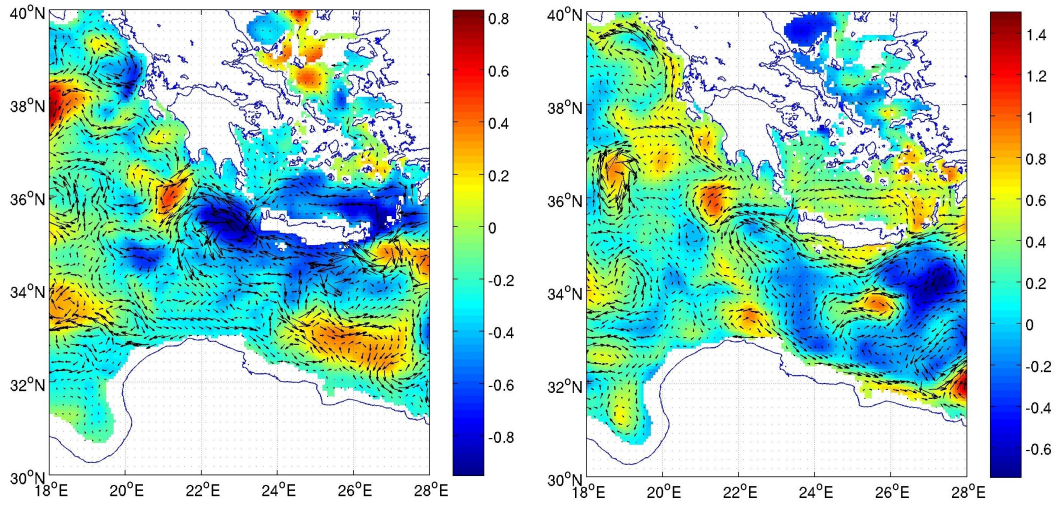


Figure 3.5: From left to right: temperature anomaly in May 1997 and in February 2004

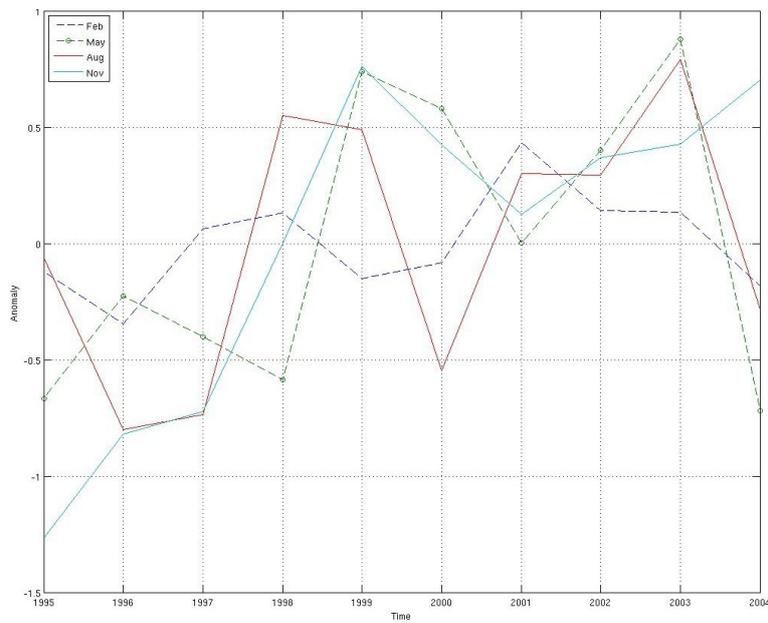


Figure 3.6: Plot of the temperature anomaly at the surface

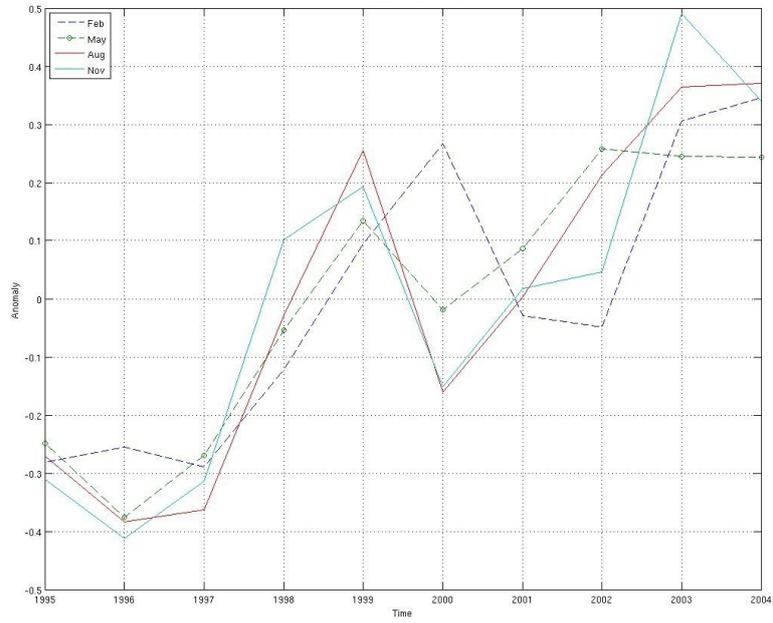


Figure 3.7: Plot of the temperature anomaly at 250 m in the Pelops Gyre area

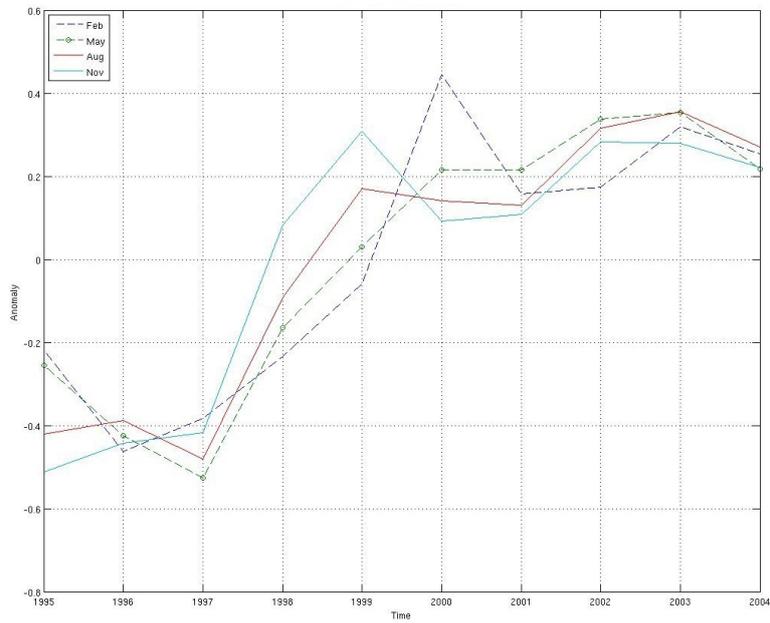


Figure 3.8: Plot of the temperature anomaly at 250 m in the Cretan Gyre area

### 3.3 Velocity Structure

The Pelops Gyre has been documented to be a recurrent large eddie. By the analysis of the horizontal velocity field it is possible to attest that during 1995-2004 both the Pelops Gyre and the Cretan Gyre are recurrent.

The Pelops Gyre is semi-permanent and tends to move towards south-west during the ten years of analysis. Furthermore, it is characterized by large interannual variability: the most extreme signals are found in November 1998, February and August 2000, February 2001, May and August 2002 and finally in August and November 2003. On the other hand, the Cretan gyre, although it is more permanent than the Pelops Gyre, shows a weaker velocity field without extreme signals throughout the overall period.

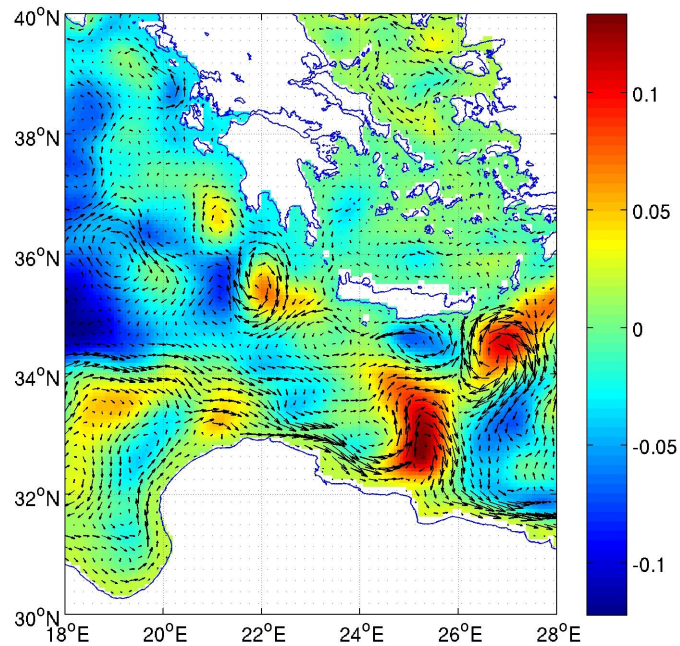


Figure 3.9: Velocity field in November 1998

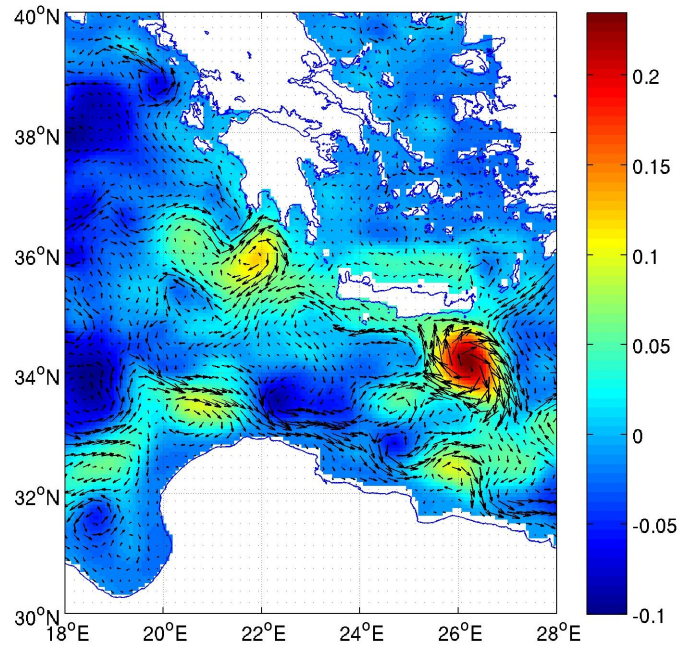


Figure 3.10: Velocity field in February 2000

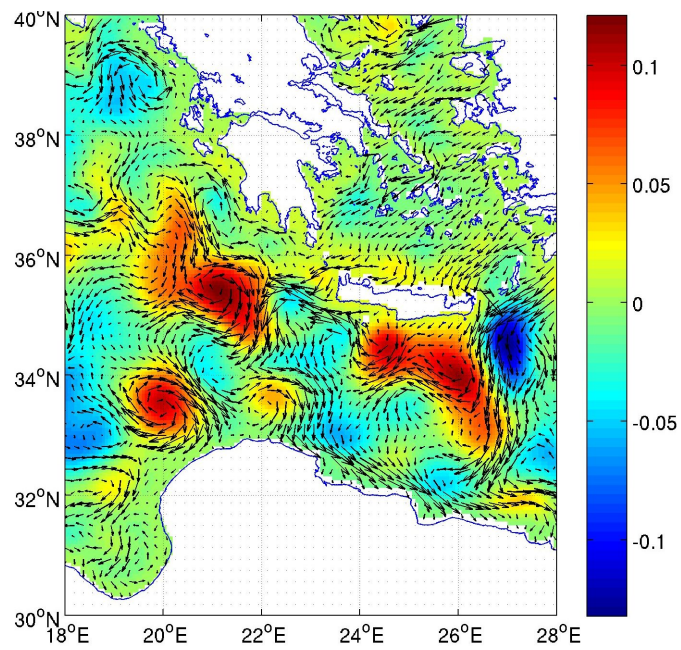


Figure 3.11: Velocity field in August 2000

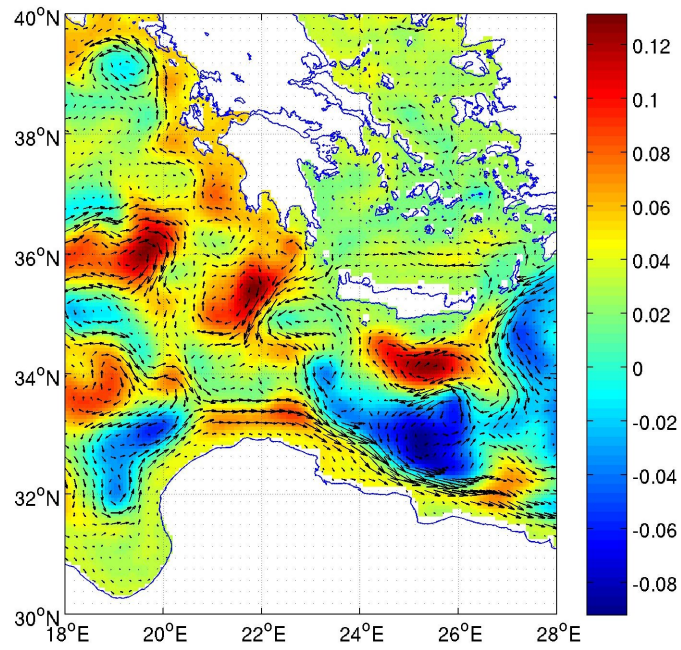


Figure 3.12: Velocity field in February 2001

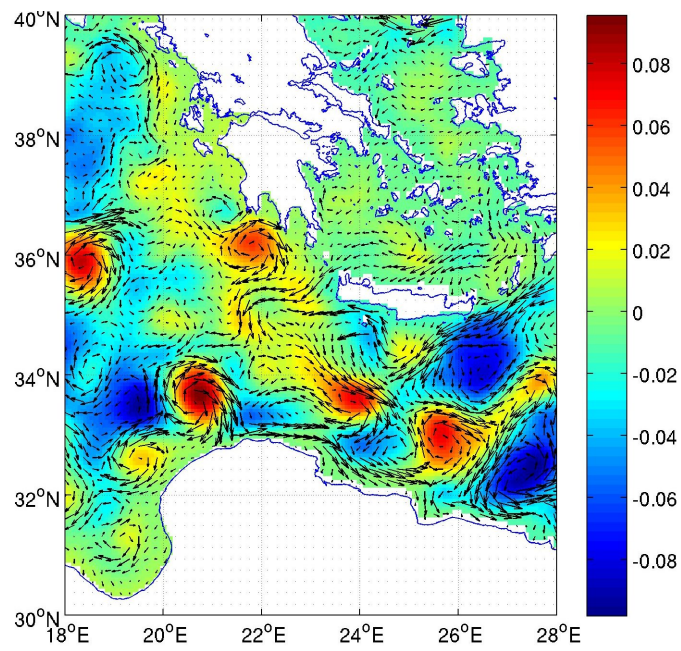


Figure 3.13: Velocity field in May 2002

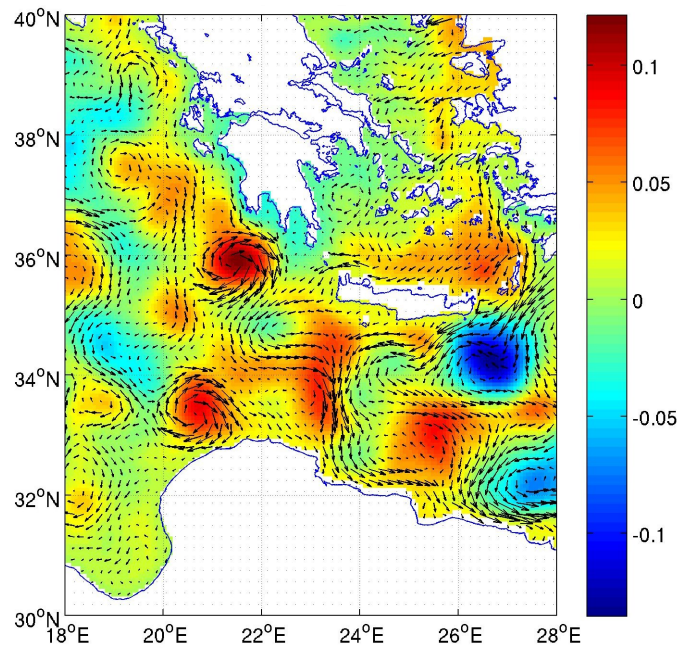


Figure 3.14: Velocity field in August 2002

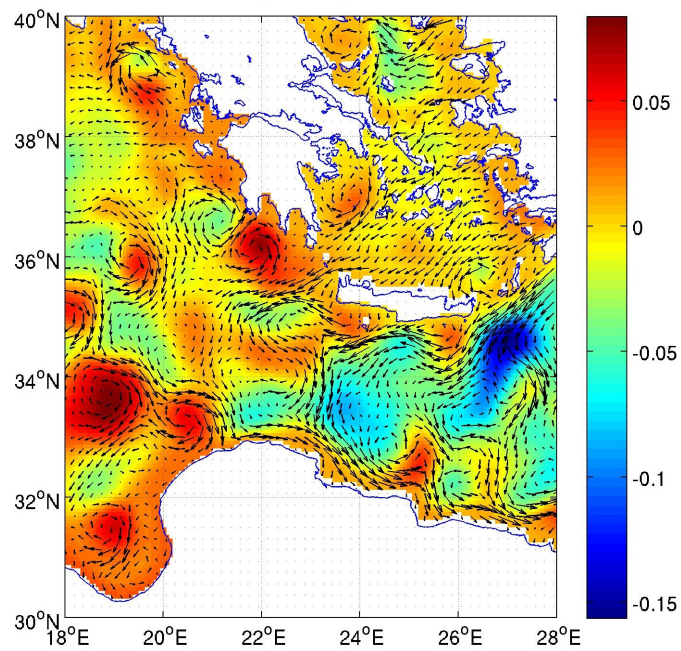


Figure 3.15: Velocity field in August 2003

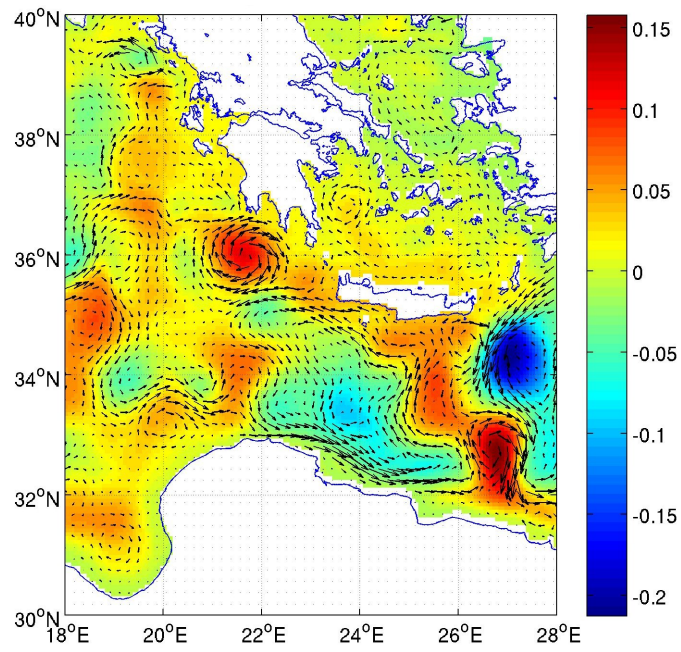


Figure 3.16: Velocity field in November 2003

### 3.4 Sea Surface Height

Sea level defines the paths of the geostrophic current at the surface with reference to a fixed surface height. By analyzing variations from this reference point, scientists determine ocean circulation and seasonal or interannual variations. The main cause of this phenomenon is attributed to the thermal expansion of the world ocean. The thermal expansion theory of the mean sea level variation is based on the fundamental physical property of seawater density to decrease or increase when heat is added or removed (Antonov et al., 2002).

In the Mediterranean Sea, it has been verified (Larnicol et al., 1995) that the sea level has a seasonal cycle: specifically the sea level is highest in October, after that it decreases rapidly until March and then rise again but more slowly.

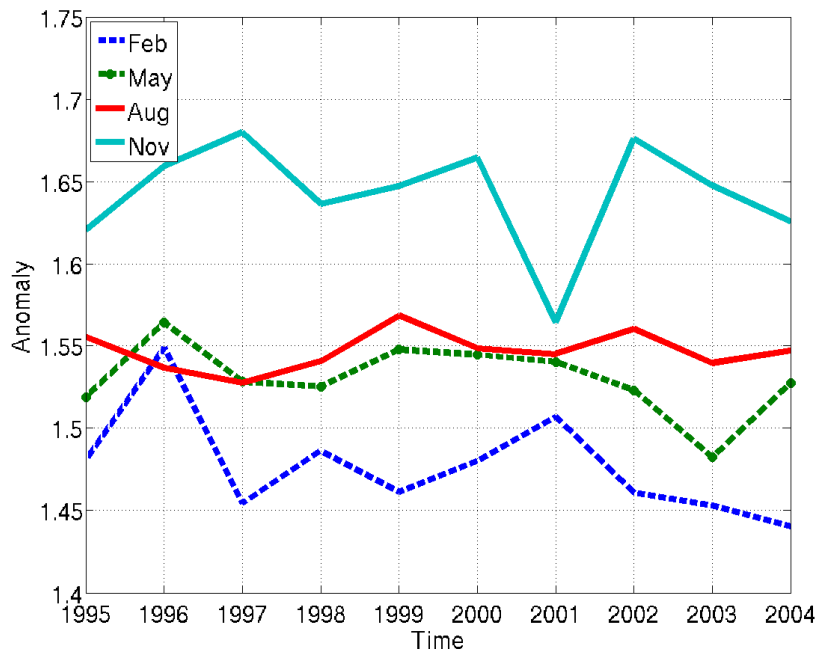


Figure 3.17: Plot of SSH anomaly in February, May, August and November during the 10 years

The plot of the SSH anomaly of the area where the Pelops Gyre and the Cretan Gyre are located (see Fig.2.1) shows that the mean sea level is highest in summer (November) and reaches its lowest values in winter (February), after that it increases gradually in May and August. Thus the mean sea level variations are attributable to the steric sea level changes in turn due to the seasonal heat fluxes variability. (see Fig.3.17)

### 3.5 Chlorophyll currents

Mass movements are also a major factor in ocean ecosystems. Upwelling and downwelling strongly influence the distribution and abundance of marine life: delivering oxygen to depth, distributing heat and bringing nutrients to the surface. Sea life is concentrated in the sunlit waters near the surface, but most organic matter is in deep waters and on the sea floor; when currents upwell, they flow up cold, deep and nutrient-rich water to the surface mixed layer.

As previously described, cyclones, which rotate anticlockwise in the Northern Hemisphere, cause transport of surface waters to the right away from the centre. The outward transport from the centre causes a net export of water, which must be replenished by upwelling that brings nutrients from depth to the surface. Conversely, anticyclonic systems, which rotate clockwise in the NH, transport surface waters towards the centre of the system with a net import of water. To balance the flow, downwelling must take place.

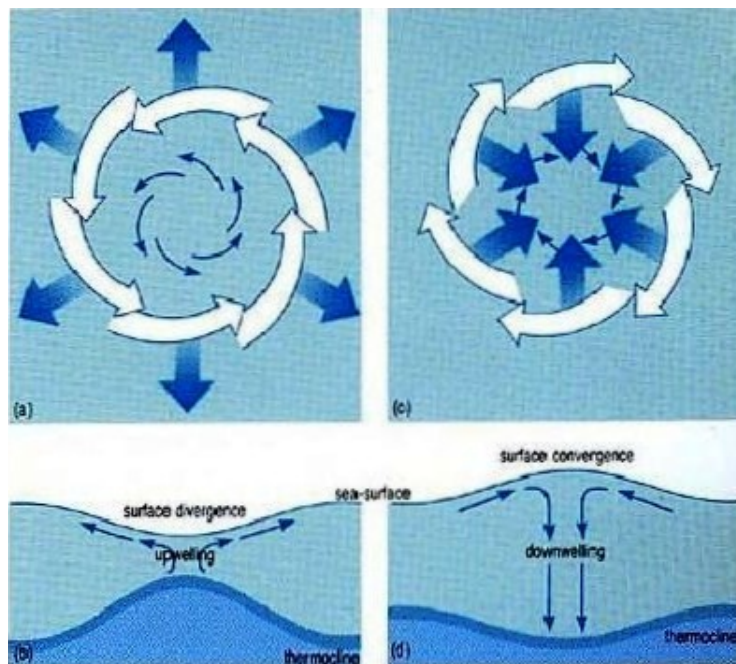


Figure 3.18: Downwelling and upwelling movements respectively in a cyclone and in an anticyclone

Therefore upwelling occurs when surface waters diverge, enabling upward movement of water and brings water that is enriched with nutrients, in fact

upwelling regions are often measured by their productivity due to the influx of nutrients to the surface layer. This drives photosynthesis of phytoplankton, which form the base of the ocean food web. On the other hand, downwelling is a kind of reverse upwelling where warm surface water sinks down to deeper depths. It occurs when surface water is forced downward by the pressure of water that forms where currents converge. Therefore, waters converge and push the surface water downwards. Regions of downwelling have low productivity because the nutrients are not continuously supplied by the cold, nutrient-rich water from below the surface.

In order to verify these processes in the studied area, the satellite chlorophyll concentration has been superimposed to the circulation structure of the two gyres. As displayed in Fig.3.19, in the core of the Pelops Gyre where the downwelling process occurs, the levels of chlorophyll are lower than the ones of the Cretan Gyre, that as cyclone, it is characterizes by upwelling.

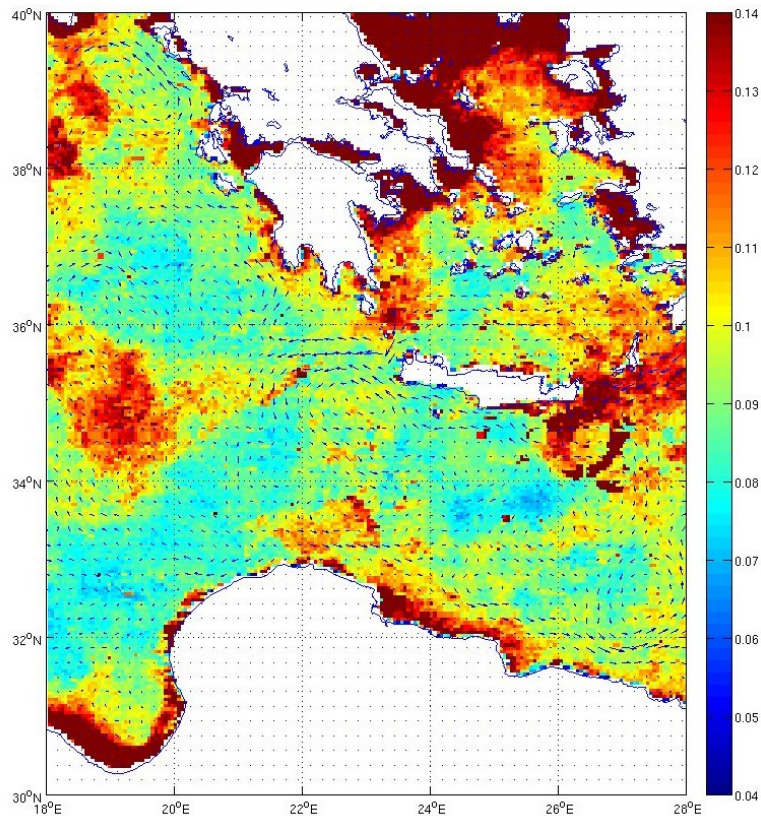


Figure 3.19: Mean phytoplankton chlorophyll concentrations ( $mgm^{-3}$ ) in the Pelops Gyre and in the Cretan Gyre.

# Chapter 4

## Conclusions

This thesis has allowed a temporal and spatial reconstruction of the two circulation structures known as the Pelops Gyre and the Wester Cretan Cyclonic Gyre between 1995-2004. In order to study their dynamics, the reanalysis datasets have proved to be valid representations of the past state of the area. As the Mediterranean Sea, the Ionian Sea circulation appears to be marked by consistent structures and strong variability. Above all, the Pelops Gyre is found to be characterized by a large interannual variability and both the two vortices can be classified as recurrent.

Furthermore, the mean sea level variations outline a seasonal cycle that is attributable to the steric sea level changes in turn due to seasonal heat fluxes variability.

Finally, satellite chlorophyll concentration levels show the occurrence of downwelling and upwelling processes in the anticyclonic and in the cyclonic core, respectively.

This thesis is only a starting point: many aspects of the Ionian Sea gyres remain unknown and several investigations still have to be carried out.

# Bibliography

- [1] Adani Mario, Dobricic Srdjan, Pinardi Nadia, *Quality Assessment of a 1985- 2007 Mediterranean Sea Reanalysis*, American Meteorological Society 2011.
- [2] Antonov John I., Levitus Sydney and Boyer Timothy P., *Sea level variations during 1957- 1994: Importance of salinity*, Journal of Geophysical Research, vol. 107, n°. C12, 8013, doi:10.1029/2001JC000964, 2002.
- [3] Ayoub Nadia, Le Traon Pierre-Yves, De Maey Pierre, *A description of the Mediterranean surface variable circulation from combined ERS-1 and TOPEX/POSEIDON altimetric data*. Journal of Marine Systems 18 (1998) 3-40.
- [4] Dobricic Srdjan, Pinardi Nadia, Testor Pierre , Send Uwe, *Ionian Sea circulation as clarified by assimilation of glider observations*.
- [5] Fusco, Manzella, Cruzado, Gasparini, Millot, Tziavos, Velasquez, Walne, Zervakis and Zodiatis, *Variability of mesoscale features in the Mediterranean Sea from XBT data analysis* Annales Geophysicae (2003) 21: 21- 32 European Geosciences Union 2003.
- [6] Grandi Alessandro, Drudi Massimiliano, Fratianni Claudia, Girardi Giacomo, Simoncelli Simona, Tonani Marina, 2014. *Product user manual for Mediterranean Sea Physical Reanalysis Product*.
- [7] International Hydrographic Organization, 1953. *Limits of oceans and seas*.
- [8] Larnicol Gilles, Le Traon Pierre-Yves, Ayoub Nadia, De Mey Pierre, *Mean sea level and surface circulation variability of the Mediterranean Sea from 2 years of TOPEX/POSEIDON altimetry*, Journal of Geophysical Research, vol. 100, n° C12, pages 25,163- 25,177, December 15, 1995.

- [9] Lascaratos Alex , William G. Richard, Tragou Elina, *A Mixed-Layer Study of the Formation of Levantine Intermediate Water*, , Journal of Geophysical Research, vol. 98, no. C8, pages 14,739-14,749, August 15, 1993.
- [10] Malanotte-Rizzoli Paola, Hecht Artur, *Large-scale properties of the Eastern Mediterranean: a review*, Oceanologica Acta 1998- vol. 11- n° 04.
- [11] Malanotte-Rizzoli et al., *A synthesis of the Ionian Sea hydrography, circulation and water mass pathways during POEM Phase I*, Progr. in Oceanography , 39, 153- 204, 1997.
- [12] Millot C. , Candelab J., Fudac J., Tberd Y., 2005. *Large warming and salinification of the Mediterranean outflow due to changes in its composition*. Deep-Sea Research I 53 (2006) 656-666.
- [13] Nittis Kostas, Pinardi Nadia, Lascaratos Alex, *Characteristics of the Summer 1987 Flow Field in the Ionian Sea*, Journal of Geophysical Research, vol. 98,n° C6, pages 10,171-10,184, June 15, 1993.
- [14] Pascual A., , Pujol MI, Larnicol G, Traon PY Le, Rio MH, *Mesoscale mapping capabilities of multisatellite altimeter missions: first results with real data in the Mediterranean Sea*,Journal of Marine Systems 65 (2007), 190- 211.
- [15] Pinardi N., Fratianni C., Adani M., *Use of real-time observations in an operational ocean data assimilation system: the Mediterranean case*.
- [16] Pinardi Nadia, Navarra Antonio, *Baroclinic wind adjustment processes in the Mediterranean Sea*, Deep-Sea Research II, Vol. 40, n° 6, pp. 1299-1326, 1993.
- [17] Pinardi Nadia, Zavatarelli Marco, Adani Mario, Coppini Giovanni, Fratianni Claudia, Oddo Paolo, Simoncelli Simona, Tonani Marina, Lyubartsev Vladislav, Dobricic Srdjan, Bonaduce Antonio, *Mediterranean Sea large-scale low-frequency ocean variability and water mass formation rates from 1987 to 2007: A retrospective analysis*, Prog. Oceanogr. (2013), <http://dx.doi.org/10.1016/j.pocean.2013.11.003>.
- [18] Robinson A.R. , Malanotte-Rizzoli, Hecht, Michelato, Roether, Theocharis, Pinardi Artegiani, Bergamasco, Bishop, Brenner, Christianidis, Gacic, Georgopoulos, Golnaraghi , Hausmann, Junghaus k,

- A. Lascaratos, Latif, Leslie, Lozano, Oguz, Ozsoy, Papageorgiou, Paschini, Rozenroub, Sansone, Scarazzato, Schlitzer, Spezie, Tziperman, Zodiatis, Athanassiadou, Gerges, Osman, *General circulation of the Eastern Mediterranean*, Earth-Science Reviews, 32 (1992) 285-309.
- [19] Robinson A.R., Leslie Wayne G., Theocharis Alexander, Lascaratos Alex, *Mediterranean Sea Circulation*, Academic Press 2001.
- [20] Roussenov Vassil, Stanev Emil, Artale Vincenzo, Pinardi Nadia, *A seasonal model of the Mediterranean Sea general circulation*, Journal of Geophysical Research, vol. 100, n° C7, pages 13,515- 13,538, July 15, 1995.
- [21] Volpe Gianluca, Tronconi Cristina, Santoleri Rosalia, Colella Simone, Forneris Vega, Bohm Emanuele, Garnesson Philippe, Malcolm Taberner, Silvia Pardo, *Product User Manual for all Ocean Colour Products*.
- [22] Wu Peili, Haines Keith, *The general circulation of the Mediterranean Sea from a 100-year simulation*, Journal of Geophysical Research, vol. 103, n° C1, pages 1121-1135, January 15, 1998.